Response Surface Methodology as a powerful tool to optimize the synthesis of polymer-based graphene oxide nanocomposites for simultaneous removal of cationic and anionic heavy metal contaminants

Jem Valerie D. Perez[a,b], Enrico T. Nadres[b], Hang Ngoc Nguyen[b], Maria Lourdes P. Dalida[a], and Debora F. Rodrigues[b*]

Supporting Information

Characterization of GO

Raman spectroscopy was used to study the structural changes and configurations of graphite and GO, as shown in SI Figure S1 (b). The G band is assigned to first-order scattering of the E_{2g} from the sp^2 hybridized carbon while the D bands is due to the defects or structural imperfections present on the graphite plane[36, 37], both are used to characterize graphene-based materials. Characteristic G peak at 1580 cm^{-1} is observed for graphite, with an almost absent D peak suggesting no defects on the carbon basal plane. On the other hand, G and D peaks at 1602 and 1350 cm^{-1}, respectively, are observed for GO, which are consistent with the well-known GO Raman peaks. The large D peak of GO denotes the significant presence of many functional groups formed.[37]

To investigate the functional groups present on the synthesized GO, FTIR analyses were performed. As shown in SI Figure S1 (c), graphite was successfully oxidized as indicated by the characteristic peaks at 3385, 1728, 1628, and 1053 cm^{-1} present in the IR spectrum of GO. These peaks are assigned to the O-H stretching of the hydroxyl groups, C=O stretching of the carboxyl groups, C=C on the hexagonal plane, and C-O of the epoxide groups, respectively.[35, 36] The presence of these functional groups confirms that GO was synthesized successfully.

Finally, XPS analysis was also performed to investigate surface composition and to further confirm the FTIR results. SI Figure S2 (a) shows wide scan spectra of graphite and GO, where a significant increase in

the O1s peak of GO is observed. Calculated C/O atomic concentration ratios of 43.4 and 1.6 for graphite and GO, respectively, confirms the successful oxidation of graphite. Furthermore, SI figure S2 (b) shows the deconvolution of the C1s core spectrum of GO. Three peaks can be observed at binding energies of 284.8 eV (C-C/C=C), 286.9 eV (C-O), and 288.5 eV (C=O)[51], which are in good agreement with the functional groups observed from the FTIR analysis.

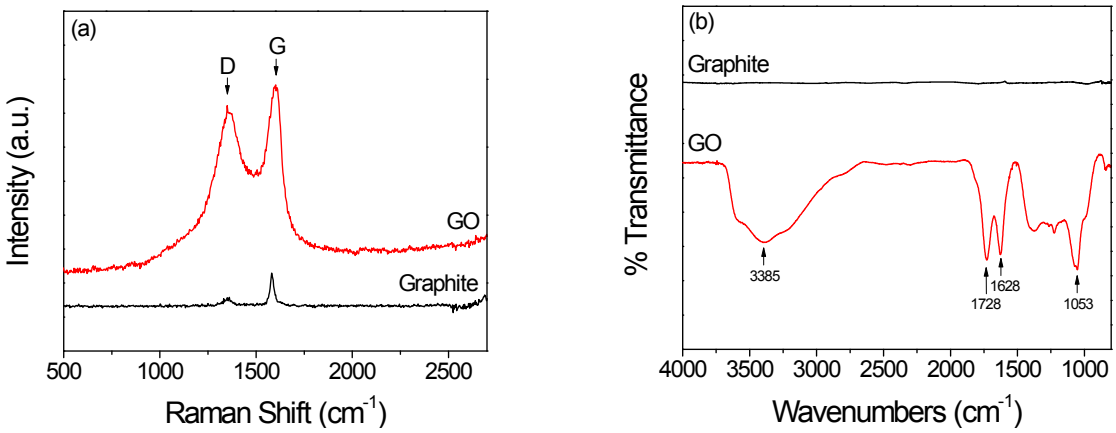

Figure S1. (a) Raman, and (b) FTIR spectra of graphite and GO

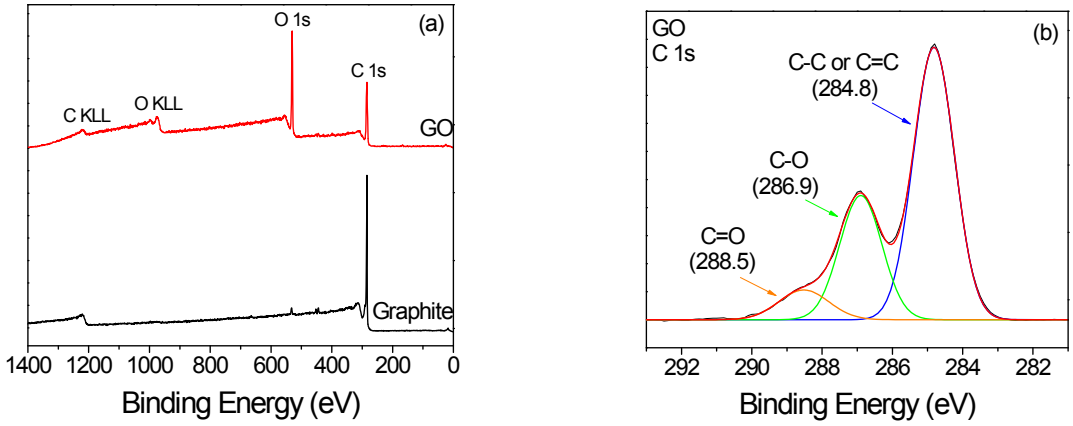

Figure S2. XPS (a) wide scan spectra of graphite and GO and (b) C1s core spectrum of GO

Data, ANOVA, and Residual Diagnostics of RSM Models

Table S1. Experimental Design Matrix with Actual and Predicted Responses

Run	X_1, PEI concentration (%)	X_2, GO concentration (ppm)	X_3, GLA concentration (%)	Y_1, % Cr (VI) Removal		Y_2, % Cu (II) Removal	
				Actual	Predicted	Actual	Predicted
1	1.00	500.00	1.50	84.0824	84.5506	61.9981	59.0063
2	1.50	1000.00	1.50	78.6517	79.3383	59.9883	64.1957
3	2.00	1500.00	1.50	89.1386	88.6704	79.6470	77.2674
4	1.50	500.00	2.50	84.2697	84.3867	52.8630	52.2379
5	1.50	1500.00	0.50	77.5281	77.3174	76.1392	76.1535
6	2.00	1000.00	2.50	88.2022	87.5702	69.0138	65.3095
7	1.50	1000.00	1.50	79.9625	79.3383	62.1442	64.1957
8	2.00	500.00	1.50	83.5206	83.7547	57.9421	63.5373
9	1.50	1500.00	2.50	85.9551	86.8680	67.5157	65.9679
10	1.50	500.00	0.50	75.6554	74.8361	68.8311	62.4235
11	2.00	1000.00	0.50	77.1536	78.0197	75.0064	75.4951
12	1.00	1500.00	1.50	84.8315	84.5974	73.2525	72.7364
13	1.00	1000.00	0.50	76.2172	76.3811	69.1965	70.9641
14	1.00	1000.00	2.50	86.3296	85.9316	59.0383	60.7785
15	1.50	1000.00	1.50	79.4007	79.3383	61.8884	64.1957

Table S2. ANOVA for Cr (VI) removal

Source	Sum of Squares	df	Mean Square	F-value	p-value Prob > F	
Model	278.79	9	30.98	37.94	0.0004	Significant
x_1 (PEI)	5.37	1	5.37	6.58	0.0504	
x_2 (GO)	12.31	1	12.31	15.08	0.0116	
x_3 (GLA)	182.43	1	182.43	223.42	< 0.0001	
x_1x_2	5.93	1	5.93	7.26	0.0431	
x_1x_3	0.22	1	0.22	0.27	0.6265[n]	
x_2x_3	8.767E-003	1	8.767E-003	0.011	0.9215[n]	
x_1^2	47.57	1	47.57	58.26	0.0006	
x_2^2	22.45	1	22.45	27.49	0.0033	
x_3^2	3.35	1	3.35	4.10	0.0988	
Residual	4.08	5	0.82			
Lack of Fit	3.22	3	1.07	2.48	0.3003	Not significant
Pure Error	0.87	2	0.43			
Cor Total	282.88	14				

[n] not significant

Table S3. ANOVA for Cu (II) removal

Source	Sum of Squares	df	Mean Square	F-value	p-value Prob > F	
Model	771.54	9	85.73	8.68	0.0142	Significant
x_1 (PEI)	41.06	1	41.06	4.16	0.0971	
x_2 (GO)	377.03	1	377.03	38.16	0.0016	
x_3 (GLA)	207.49	1	207.49	21.00	0.0059	
x_1x_2	27.30	1	27.30	2.76	0.1573[n]	
x_1x_3	4.34	1	4.34	0.44	0.5369[n]	
x_2x_3	13.49	1	13.49	1.36	0.2954[n]	
x_1^2	68.21	1	68.21	6.90	0.0467	
x_2^2	24.42	1	24.42	2.47	0.1768[n]	
x_3^2	21.72	1	21.72	2.20	0.1983[n]	
Residual	49.40	5	9.88			
Lack of Fit	46.63	3	15.54	11.20	0.0830	Not significant
Pure Error	2.77	2	1.39			
Cor Total	820.95	14				

[n] not significant

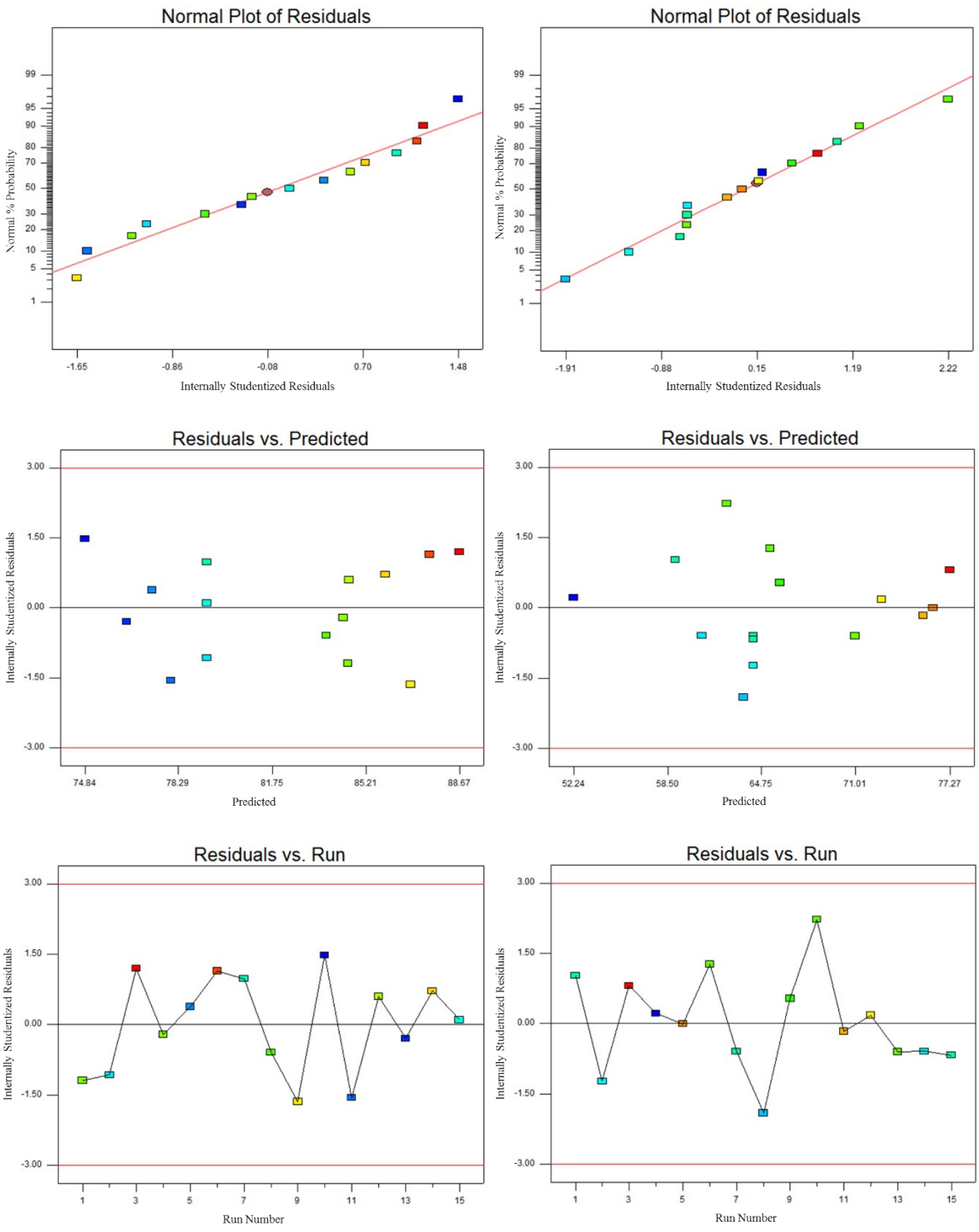

Figure S3. Residual plots for (a) Cr (VI) and (b) Cu (II) response

Macro-image and chemical stability of CS-PEI-GO beads and other control beads

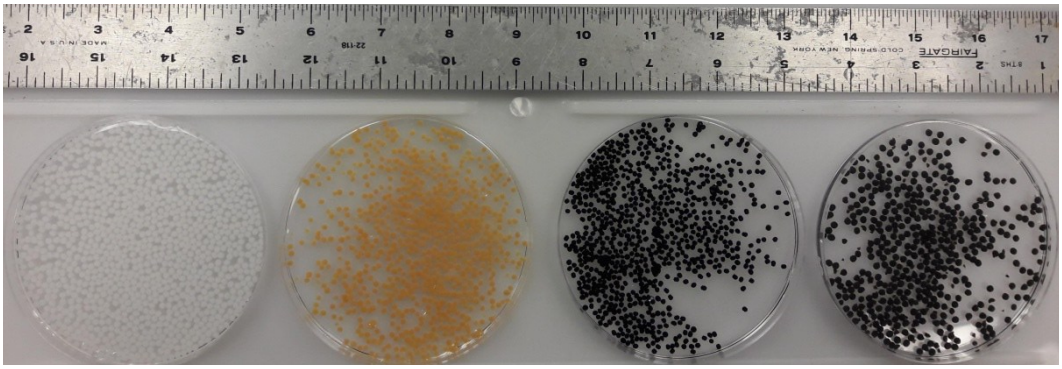

Figure S4. Spherical CS-PEI-GO beads of about 3 mm in diameter. We were able to synthesize stable CS, CS-PEI, CS-GO and CS-PEI-GO by crosslinking with glutaraldehyde.

Chemical Stability

Solubility tests with different solvents were performed and the results proved that the beads are insoluble in different acidic and basic solutions, as shown in Table S4. The good chemical stability of the beads can be attributed to the successful crosslinking reaction between GLA and the amine groups present in the beads. This stability over a wide pH range is favorable for the potential applicability of the beads to different

types of wastewaters, as well as the possibility of regeneration of the beads using different desorption agents.

Table S4. Solubility tests of CS-PEI-GO beads in different solutions

Solution	**Remarks**
0.1 M HCl	Insoluble
1 M HCl	Insoluble
0.1 M NaOH	Insoluble
1 M NaOH	Insoluble
5% acetic acid (v/v)	Insoluble